Theor Chem Acc (2010) 127:671–679
DOI 10.1007/s00214-010-0774-y

REGULAR ARTICLE

Molecular dynamics study of formamidine decomposition in gas and solution phases via free energy curves from ab initio interaction potentials

S. Tolosa Arroyo · A. Hidalgo Garcia · J. A. Sansón Martín

Received: 12 April 2010 / Accepted: 10 June 2010 / Published online: 26 June 2010

Abstract A procedure is described for the theoretical study of chemical reactions in solution by means of molecular dynamics simulation, with solute–solvent interaction potentials derived from ab initio quantum calculations. We apply the procedure to the case of the decomposition of formamidine, $HCNHNH_2 \rightarrow NH_3 + HCN$, in both gas and solution phases, via the non-assisted and assisted mechanisms. We used the solvent as reaction coordinate and the free energy curves for the calculation of the activation energies. The results showed that the decomposition assisted with one or two water molecules in aqueous solution is preferred over the non-assisted mechanism, reducing significantly the activation barrier.

Keywords Molecular dynamics simulation · Reaction mechanisms · Ab initio solute–solvent potential · Chemistry reactivity in solution

1 Introduction

Amidine compounds consist of an N–C=N framework with four possible substituents R_1, R_2, R_3, and R_4. They are of interest because of their medical and biochemical importance, having many biological and pharmaceutical uses [1, 2]. Formamidine is the simplest of the amidines (with all the R's being H) and has found major applications in synthetic organic chemistry, in the biosynthesis of important biologic compounds, and in agricultural pesticides [3]. Due to its small size, it has been employed as a test of both experimental and theoretical investigations.

In particular, formamidine has been extensively studied theoretically, especially in hydrogen-bonded complexes and in chemical reactions. The proton affinities of amidines [4], tautomerization by intramolecular hydrogen transfer [5–8], hydrogen transfer in bases of nucleic acids [9], the deamination reaction to yield formamide [10], hydrolysis via different pathways [11], and decomposition at elevated temperatures yielding hydrogen cyanide and ammonia [12–17] are some of the reactions studied. Since most hydrogen transfers occur in aqueous solution, one must consider the role of water molecules in hydrogen transfer. Water can act not only as a solvent but also as a catalyst by both donating and accepting an hydrogen following an assisted mechanism path.

The unimolecular decomposition mechanism of the Z-isomer of formamidine to give ammonia and hydrogen cyanide has been investigated experimentally [12] and theoretically [13–17] by several workers. Most of them considered the gas-phase reaction [13–15], while others take into account the mechanism in solution assisted by one or more molecules of water [16, 17]. The work of Andres et al. [13, 14] presents ab initio HF studies in gas phase with small bases and considering only one transition state formed by a four-membered ring, while the work of Kaushik et al. [15] extended the study to other levels such as MP2 and B3LYP calculations with 6-31G* bases, with both studies finding very high activation barriers. The work of Almatarneh et al. [16] deals with the study of the decomposition reaction in gas and solution phases but considers the solvent as a continuum using the PCM model

Electronic supplementary material The online version of this article (doi:10.1007/s00214-010-0774-y) contains supplementary material, which is available to authorized users.

S. T. Arroyo (✉) · A. H. Garcia · J. A. S. Martín
Departamento de Química Física,
Universidad de Extremadura, 06071 Badajoz, Spain
e-mail: santi@unex.es

[18]. Those authors analyze the reduction in the activation barrier when one or two water molecules are involved in the reaction mechanism. Using MP2 and high levels of the Gaussian-n theory [19], they improve the results of the activation barrier of previous studies but are still far from experimental results. There has been only one study for this reaction in solution using a discrete model to describe the surrounding environment, in which the solvent effects were been investigated for formamidine bonded to a water molecule using a chemical molecular dynamic simulation method [17]. In this case, the results were more consistent with the available experimental data.

The gas-phase unimolecular decomposition of Z-isomer formamidine leads to a transition state TS0 formed by a shift of the hydrogen from the imino nitrogen to the amino nitrogen which continues with the breaking of the N···C and N···H bonds to give the products (Scheme 1). When the reaction is assisted by water molecules, the mechanisms are similar to that mentioned above, although now the water molecules are involved in the TS1 and TS2 transition states (of six- and eight-membered rings when one or two water molecules are participating, respectively, in the mechanism). The participation of three molecules of water in the reaction mechanism was not considered due to its not reducing the activation barrier, since the formation of a transition state of ten members is an entropically unfavored process.

However, in solution the decomposition reaction of formamidine involves a two-step mechanism: (a) a first step where the TS0, TS1, and TS2 transition states are formed in a way similar to the gas phase; and (b) a second step where there are formed, firstly, a zwitterionic intermediates I0, I1, and I2, and then a second transition states TS0′, TS1′, and TS2′ close in energies to these intermediates but with the N···C single bond distance and H–C=N angle somewhat greater, before obtaining the ammonia and hydrogen cyanide products (Scheme 2).

As the first step of this reaction mechanism is similar in both phases and is the determining factor in the rate of reaction, only the barrier energies for the TS0, TS1, and TS2 states in gas and solution are studied in this paper.

The thermodynamic study of the decomposition of formamide can lead to different results depending on the type of calculation. Thus, ab initio calculations in the gas phase show that the activation barrier depends significantly on the basis and level of calculation employed [13–15]. Also the result for activation energies depends greatly on the method used to include the solvent effects: molecular mechanics (MM), polarizable continuum model (PCM), quantum mechanics/molecular dynamics (QM/MD), molecular dynamics (MD), etc.

Continuing in the line of our studies of chemical reactivity in solution using the MD/ESIE method [20–22], described below in the section "Formalism and Calculation Details", which has so far been applied to hydrolysis reactions, we here apply it to the formamidine decomposition reaction in solution. Our goal is to show the improvement in the results when the solvent is not described as a continuum but as a discrete system formed by numerous water molecules interacting with the solute (reactants and transition states). This method differs from that used by Ando and Hynes in the ionization reaction of acids [23], in that it uses potentials in which the interaction parameters were obtained from ab initio calculations

Scheme 1 Decomposition of formamidine in the gas phase

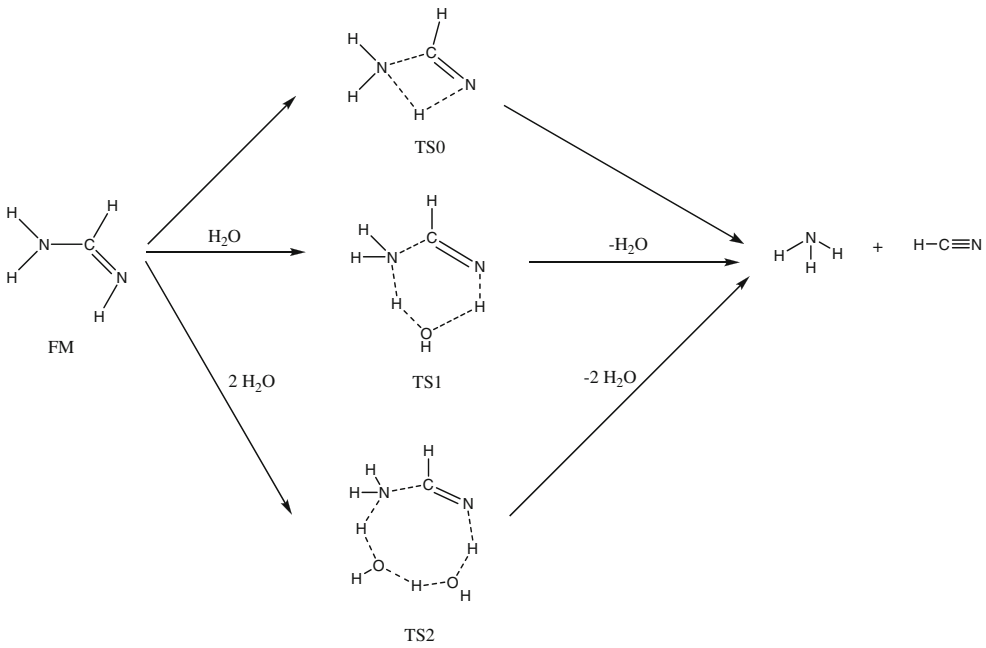

Scheme 2 Decomposition of formamidine in solution phase

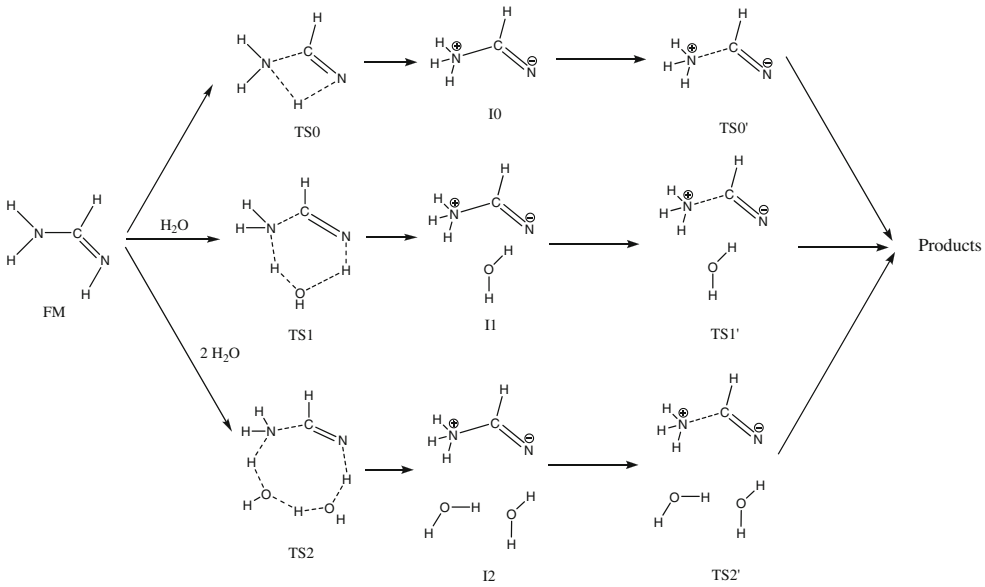

instead of using Lennard-Jones parameters, and in the way it obtains the free energy curves in zones away from the minimum.

Given this context, the general objective of the present study is to show that the form of obtaining the free energy curves via the MD/ESIE with a discrete solvent model seems in general sound and provides a reasonable option within the present limitations of the MD simulation. In particular, the detailed objectives are to: (a) apply the methodological approach based on free energy curves to this decomposition reaction to provide values of activation free energies in solution; (b) compare our MD results from free energy curves with those existing in the literature from other methods used in the study of reactions in solution; (c) obtain the structures of different transition states in solution using PCM and/or QM/MM models, comparing our results with others that are available; and (d) illustrate the advantages of using free energy curves obtained from molecular dynamic to study reactions in solution instead of using the free energy for each individual specie in the reaction.

2 Formalism and calculation details

About a thousand values of the SCF and MP2 solute–solvent interaction energy U_{sw} were calculated with the 6-311++G** basis [24, 25] and considering the BSSE effect [26]. To generate the grid of points, the water molecule was placed in different positions r_{ij} with respect to the solute, trying to describe adequately the attractive, repulsive and long-range interactions. Starting with a separation of at least 1.5 Å from any solute atom, the positions x, y, and z for each configuration were increased in steps of 0.5 Å. With regard to the basis used, the 6-311++G** basis set contains not only polarization functions in all of the atoms, but also diffuses functions to improve the description of the outermost orbital and thereby of the reactant and transition state energies and geometries, because a previous study [27] showed the importance of these functions in the construction of the free energy curves using the method of the present work.

These energies were used to obtain the A_{ij}, B_{ij}, and q_i interaction parameters of the potential function used in our calculations:

$$U_{sw} = \sum_{ij} \frac{A_{ij}^{sw}}{r_{ij}^{12}} - \sum_{ij} \frac{B_{ij}^{sw}}{r_{ij}^{6}} + \sum_{ij} \frac{q_i^s q_j^w}{r_{ij}} \quad (1)$$

The net charges on each solute atom q_i^s were obtained with the ESIE procedure [28], fitting the values of the Coulomb component of the interaction energy $U_{sw}(ES)$ with values $\leq$5 kcal/mol using the variational scheme of Morokuma and coworkers [29, 30]:

$$U_{sw}(ES) = \sum_{ij} \frac{q_i^s q_j^w}{r_{ij}}, \quad (2)$$

where the charges of the solvent water q_j^w are pre-assigned as the TIP3P charges [31].

The Lennard-Jones parameters A_{ij}^{sw} and B_{ij}^{sw} are obtained in a similar way to q_i^s, but now the energies used in the fits are those with values $\leq$10 kcal/mol that describe the exchange (EX) and polarization (PL) components of the interaction energy at the SCF level, and the dispersion (DIS) component related to the MP2 correlation energy:

$$U_{sw}(EX) = \sum_{ij} \frac{A_{ij}^{sw}}{r_{ij}^{12}}. \quad (3)$$

$$U_{sw}(PL + DIS) = -\sum_{ij} \frac{B_{ij}^{sw}}{r_{ij}^{6}}. \quad (4)$$

To construct free energy curves G, we use as reaction coordinate the difference in the interaction energy of a given set of solvent molecules in the presence of the reactant and transition-state structures [32], for which one only needs the potential function that suitably describes this interaction. This reaction coordinate is widely used in electron transfer reactions, although it has also been successfully used in atom transfer reaction (such as hydrogen transfer) [23, 33–35].

Thus, to obtain the curve associated with the reactant simulation G_R one can use the differences in the solute–water interaction energies, (U_{sw}), between the diabatic states of the solute in its reactant (R) and transition-state (TS) structures for a broad set of configurations of solvent molecules around the solute in a molecular dynamics simulation of the reactant solvation:

$$\Delta E_R = U_R(W, S_R) - U_R(W, S_{TS}) \quad (5)$$

where $U_R(W,S_R)$ denotes the total potential energy including the solute internal energy $U_{int,R}$, the solute–solvent interaction $U_{SW,R}$, and the solvent–solvent interaction $U_{WW,R}$ at a fixed solute coordinate S_R, as a function of the solvent configuration W.

One operates in a similar way to simulate the solvation of the transition state and to obtain the ΔE_{TS} values with respect to the other system, considering the same direction in all the cases, i.e. $\Delta E_{TS} = U_{TS}(W, S_R) - U_{TS}(W, S_{TS})$.

The difference ΔE_s fluctuates during the s simulation, and its values are collected as a histogram of the number of times that a particular value Δe of the macroscopic variable ΔE_S appears in the simulation. The probability $P_s(\Delta e)$ of finding the system in a given configuration can be expressed in terms of the delta function δ described in previous works [20–22, 36, 37] and of the number of equally spaced steps N_s in the simulation:

$$P_S(\Delta e) = \frac{\sum_{i=1}^{N} \delta(\Delta E_s(t_i) - \Delta e)}{N_s}. \quad (6)$$

This allows us to compute the free energy $G_S(\Delta e)$:

$$G_S(\Delta e) = -k_B T \ln P_S(\Delta e). \quad (7)$$

Next, a search is made for the polynomial function that best fits these free energies and the result is plotted as G_s. In practice, only a small region of these curves around the minimum of G_s is obtained, whereas high free energy regions near the diabatic crossing are also important to obtain the activation barriers. In our procedure, we fit these energies to polynomial functions using different energies $G_s(\Delta e)$, although other methods can be applied (free energy perturbation method [36, 37] and Tachiya's procedure [38]).

In all cases, the separation between the two minima determines the activation barrier:

$$\begin{aligned} \Delta G^{\neq} &= G_{eq}^{TS} - G_{eq}^{R} \\ &= a(\Delta e_{eq}^{TS} - \Delta e_{eq}^{R}) + b(\Delta e_{eq}^{TS} - \Delta e_{eq}^{R})^2 \\ &\quad + c(\Delta e_{eq}^{TS} - \Delta e_{eq}^{R})^3 + \ldots \end{aligned} \quad (8)$$

with Δe_{eq}^{R} and Δe_{eq}^{TS} being the most probable values of ΔE in the free energy curves G_R and G_{TS}, respectively, and a, b, and c are the coefficients of the polynomial fit to the curve G_R.

The advantage of this procedure of using the minima of the G_R and G_{TS} curves obtained from simulations of the two systems, and the a, b, and c coefficients from the polynomial fit to the curve G_R, relative to other methods [38] in which the curves are moved seeking to connect smoothly the different curves G's curves obtained from the relationship $G_S' = G_S \pm \Delta e$, is that the result of the activation barrier is independent of the displacement of those curves. Moreover, the use of Eq. (5) implies that the activation barrier is independent on the solvent–solvent energies (these energies cancel out for each G_s curves) and of the solute intramolecular energy (this energy cancels out when comparing the G_R and G_{TS} curves).

Once the G_R and G_{TS} curves have been obtained to display the activation barrier, one needs to displace the curves to a point where Marcus's relation is satisfied:

$$\Delta G^{\#} = \frac{(\Delta G + \lambda)^2}{4\lambda}, \quad (9)$$

which in the case of this R → TS step with no activation barrier ($\Delta G^{\#} = 0$) is equivalent to the energy of the process matching the solvent reorganization energy ($\Delta G = -\lambda$), and to shifting the G_R curve seeking to cross the G_{TS} curve at the minimum.

When calculating the energy differences ΔE_s between the solutes and the water solvent, and then constructing the ΔG_s free energy curves, it must be taken into account that it is necessary during the simulation of one of the solutes to displace the other solute to the position occupied by the first and to reorient it in order to reproduce the position of their atoms. In the case of a reaction such as the present R → TS, with one solute molecule and one or two water molecules, one must choose correctly the separation between the solute and the water molecules in order to carry out the simulation, since the solute–solvent

interaction energies will depend notably on the separation and orientation of these molecules. We consider the case where the intermolecular separation distance between formamidine and water molecules is similar in the reactant and in the transition state, to facilitate the molecular superpositions. In this way, the differences between the solute internal energies are small when going from reactant to transition state. Once these simulations are complete and we have thousands of solvent configurations, molecular superpositions are performed between the reactants and the transition state to obtain the G_R curve according to Eq. (5). One proceeds similarly to construct the G_{TS} curve but simulating the transition state in solution and superposing the reactant system.

Finally, some simulation details merit commentary. Molecular dynamics simulations of an NVT ensemble of a solute molecule in an aqueous environment formed by about 205 water molecules were carried out at 298 K using the AMBER program [39]. The time considered for the simulations was 2,000 ps with time steps of 0.1 fs. The first 1,000 ps were used to ensure that the equilibrium is reached completely, and the last 1,000 ps were to store the configurations of the water molecules required for the determination of the thermodynamic properties studied in this work. The water molecules initially located at distances less than 1.6 Å from any solute atom were eliminated from the simulations. The long-range electrostatic interactions were treated by the Ewald method [40], and the solutes were kept rigid using the shake algorithm [41]. A cutoff of 7 Å was applied to the water–water interactions to simplify the calculations, and periodic boundary conditions were imposed to describe the liquid state. The grid of points used to fit the interaction potential to the Lennard-Jones 12-6-1 function was obtained with SCF and MP2 energies using the Gaussian/98 package [42], and the decomposition of the interaction energies with the Gamess program [43].

The free energies of the individual species involved in different reaction mechanisms have been calculated with the subroutine THERMO implemented in the GAUSSIAN/98 software, for both the gas and the solution phases with the polarizable continuum model PCM [18] using the KLAMT cavity model for the geometries optimization and the SCFVAC option for the salvation energies. The QM/MM method [44–58], using the ASEP/MD code [59] that employs a mean field approximation to represent the solute–solvent interaction and the MOLDY program [60] for the molecular dynamics calculation, has been applied to locate those saddle points in solution [61] that were not found with the PCM model, using similar MD conditions to those describes in preceding paragraph.

3 Results and discussion

3.1 Transition-state structures

Ground-state geometries of the transition states in the gas and solution phases were optimized at MP2 level with the 6-311++G** basis [24, 25] starting from standard geometries. For the TS0 transition state, the geometries in solution (Fig. 1) were obtained with the PCM model. For the TS1 and TS2 transition states, where the water molecule involved in the reaction mechanism, we need to describe the solvent as a discrete medium, for which we used the QM/MM model to find those structures. All transition-state structures were confirmed by checking that

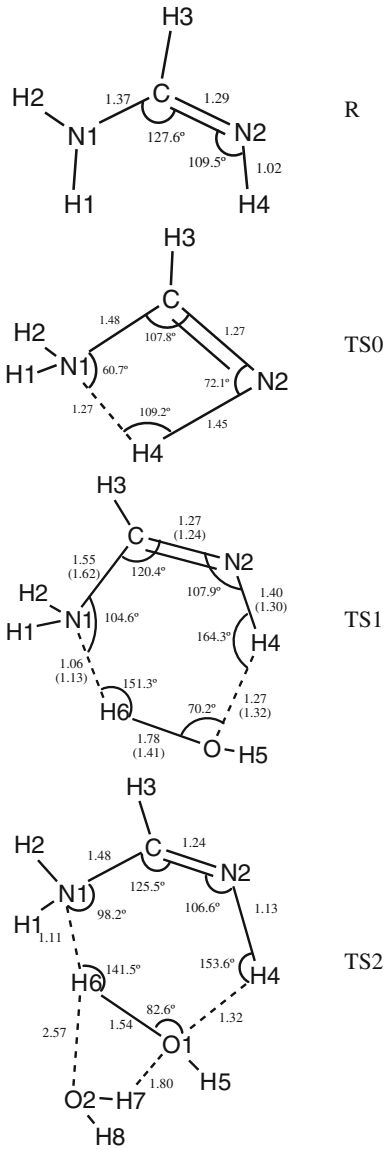

Fig. 1 Transition state geometries in solution (in parentheses, values for gas phase in the TS1 case)

there was one negative eigenvalue in the diagonalized hessian corresponding to the movement along the reaction path.

In the non-assisted mechanism, the reaction takes place with a shift of the hydrogen from the imino nitrogen to the amino nitrogen in the near-planar formamidine structure. In this process, the N2-H4 distance undergoes a significant increase from 1.02 in the reactant to 1.45 Å in the TS0 transition state which facilitates its subsequent breakage, and the H4-N2-C and N1-C-N2 angles are greatly reduced when the four-membered ring is formed. Also the N1-C distance increases by nearly 0.1 Å, and the H4 atom is close to the N1 atom in the transition-state structure, as preparation for the formation of the NH_3 and HCN products.

When the mechanism is assisted by one water molecule, the transition state with the TS1 structure is reached, and the reaction takes place with the transfer of the H4 hydrogen from the imino nitrogen to the water oxygen, and of the H6 hydrogen from the water oxygen to the amine nitrogen. In this situation, the six-membered ring formed is more flexible, and the angles are closer to those in the formamidine (FM) reactant. With respect, to the water molecule, the O-H6 distance increases to 1.78 Å and the H6-N1 distance decreases with respect to the TS0 transition state. These values confirm that the water molecule favors the proton transfer relative to the TS0 case.

As was shown in previous work [16], the assistance of a second water molecule in the transition state TS2 should lead to an eight-membered ring with increased internal angles. However, with certain basis sets and levels of calculation, the TS2 transition state, although its distances and angles are different, is similar to TS1 and to that obtained by other workers [16] in that it consists of a six-membered ring. In this case, one water molecule is involved directly in the proton transfer as part of the ring, while the other water molecule stabilizes the ring through a hydrogen bond with the ring's O1 ($R_{H7\cdots O1} = 1.80$ Å).

Finally, it should be noted that the TS1 and TS2 structures are not planar (their torsion angles are different from 0° to 180°) and the two transition states only exist when the QM/MM model is employed because with the PCM formalism, the Lennard-Jones interaction is absent. The geometrical parameters of the transition states in the gas and solution phases are similar, except for the distances of the bonds involved in the proton transfer. In particular, the hydrogen-donor (N2-H4 and O-H6) distance is greater and the hydrogen-acceptor (H6···N1 and H4···O) is smaller, favouring formamidine decomposition in the solution (see the TS1 structure values in Fig. 1). The Cartesian coordinates of these geometries are given in the supplementary material to this work.

3.2 Atomic populations

An atomic population analysis of the molecules involved in the process of formamidine decomposition showed that the net charges on atoms in solution are considerably greater than those in the gas phase (Fig. 2). Also, the charges obtained with a discrete model to describe the solvent (ESIE procedure) differ significantly from the charges with the PCM continuum model, with the greatest values being obtained with the ESIE charges, so that the proton transfer process is more favoured than in the other cases.

Comparing the ESIE atomic charges for the formamidine reactant with those in the TS0 transition state, one observes that the proton transfer process partially neutralizes the atomic charges on the reactant, resulting in less charged TS0 atoms (there is a significant decrease in the charge on the N2 and N1 atoms during this process). The analysis performed for the atoms of the TS1 and TS2 structures showed that in all cases, the H6 → N1 proton transfer in solution neutralizes the charge of the nitrogen N1, while the population increases on the oxygen (in the TS2 case, the increase is less marked due to the transfer of part of the charge to the second water molecule).

3.3 Energies

Table 1 lists the results for the activation free energies obtained for the decomposition of formamidine, in the gas and solution phases and with different mechanisms studied in this work, from the free energy curves G_R and G_{TS} given in Fig. 3 (in the three cases, the polynomial function for the curve R is shown, and for the FM + H_2O reaction, the map of energies ΔE_R is display).

In relation to the activation energy, different situations should be taken into account. First, for the case of the non-assisted mechanism, the activation barrier $\Delta G^{\neq}$ is reduced considerably when one takes into account the medium in which the reaction takes place and the model used to describe it. Thus, the energy barrier in the gas phase can be reduced from 59.33 to 54.76 kcal/mol by considering the solvent to be continuum. The reduction is even greater when the activation barrier is determined in solution using ESIE charges and free energy curves $\Delta G^{\#} = 40.02$ kcal/mol. Our PCM results are in agreement with those of previous studies in the gas phase $\Delta G^{\#} = 61.17$ kcal/mol and solution $\Delta G^{\#} = 56.91$ kcal/mol using PCM/MP2/6-31G(d) similar conditions [16], although our MD/ESIE studies give barriers smaller than these values due to the discrete description of the solvent and to the use of higher ESIE charges.

When the solvent molecules catalyze the reaction, the activation barrier is also reduced significantly. Thus, in the case of the TS1 transition state, the barrier reaches a minimum value of 22.66 kcal/mol using the present

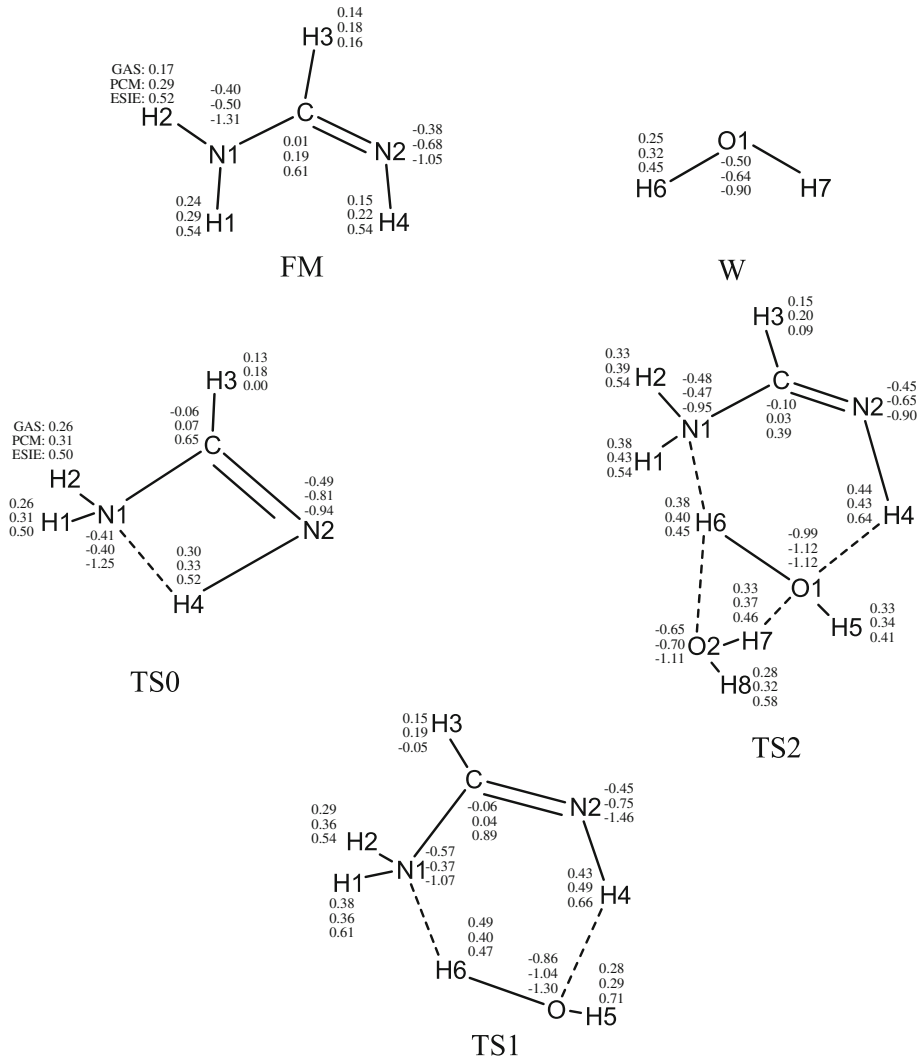

Fig. 2 Gas and solution (PCM, ESIE) charges for formamidine (FM), water (W), and transition states (TS0, TS1, and TS2)

Table 1 Activation free energies (kcal/mol) for the decomposition of formamidine (FM)

Method	$\Delta G^{\neq}$		
	FM	FM + H_2O	FM + $2H_2O$
Gas/MP2[a]	59.33 (1.9×10^{-31})[d]	43.07 (5.2×10^{-18})	40.89 (6.8×10^{-15})
Solution/PCM[a]	54.76 (7.0×10^{-26})	40.42 (7.1×10^{-17})	–
Solution/PCM[b]	56.91 (1.74×10^{-30})	36.31 (2.40×10^{-12})	–
Solution/CRMD[c]	–	15.69 ($6.31 \times 10^{+2}$)	–
Solution/MD-ESIE[a]	40.02 (2.8×10^{-17})	22.66 (4.9×10^{-3})	19.16 ($7.8 \times 10^{+1}$)

[a] Results obtained by us in this present work

[b] Results obtained by Almatarneh et al. [16] using the MP2/6-31G(d) level

[c] Results obtained by Nagaoka et al. [17] using the CRMD method

[d] Values in parentheses are rate constants in s^{-1} obtained with transition state theory

procedure (ESIE charges and free energy curves). This value is not only below that obtained without water in the mechanism, but reduced 17.76 kcal/mol relative to the PCM result. We think that this result of 22.66 kcal/mol is better than the value of 40.42 kcal/mol obtained here with the PCM (similar to the 36.31 kcal/mol obtained by Almatarneh et al. [16] with the PCM model) since the major reduction produced by the presence of water in the mechanism leads to a rate constant of $k = 4.9 \times 10^{-3}$ s^{-1} that is coherent with the rate constants of other amidine

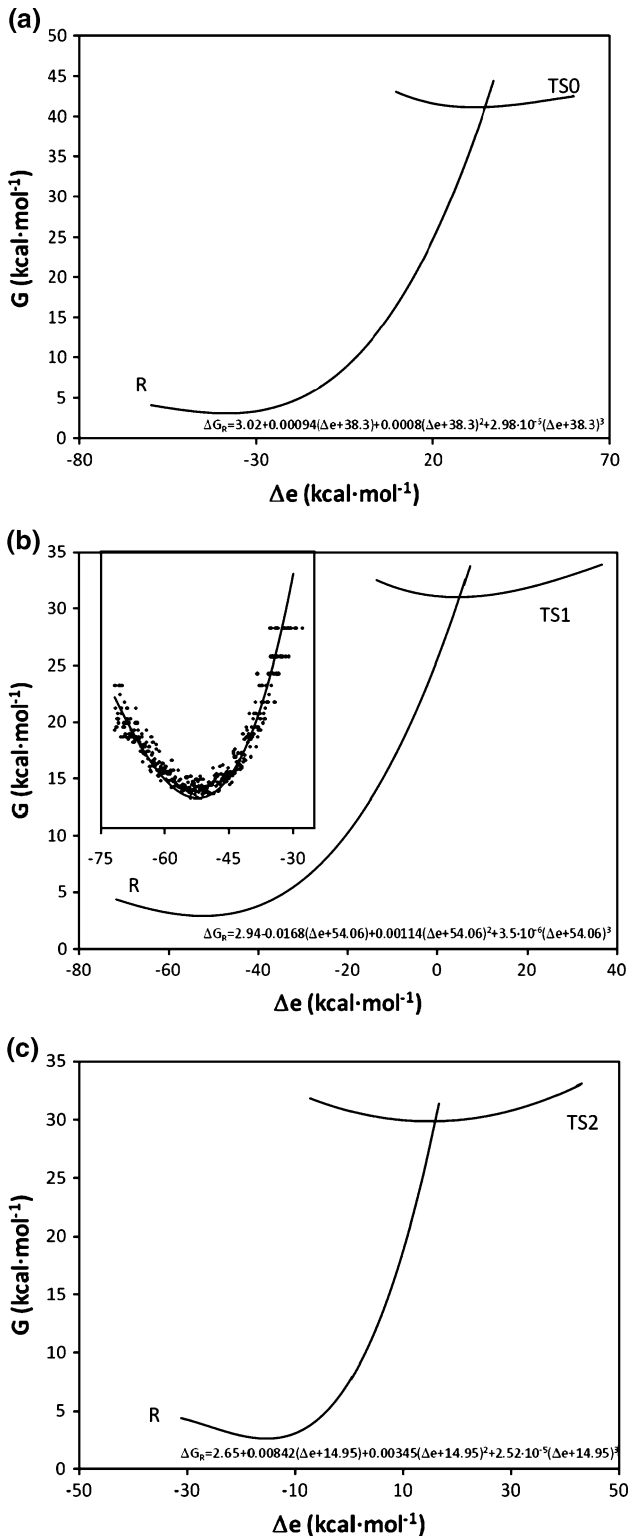

Fig. 3 R and TS free energy curves with different mechanisms

decompositions (for example, values for the DMFA hydrolysis in the range 3×10^{-5} to 3×10^{-3} s^{-1} were found [62]). Furthermore, our MD/ESIE result is in good agreement with that obtained by Nagaoka et al. of 15.69 kcal/mol using the chemical reaction dynamics method in solution [17].

Similar comments can be made when the mechanism is assisted by two water molecules, but now the activation barrier remains practically constant when the free energy curves are used, since this second water molecule is not part of the structure and only assists the reaction by forming hydrogen bonds. This result can be explained via the free energies of solvation for the transition structures: TS0 ($\Delta G_{solv} = -13.33$ kcal/mol), TS1 ($\Delta G_{solv} = -23.74$ kcal/mol), and TS2 ($\Delta G_{solv} = -14.84$ kcal/mol). When one water molecule is considered in the structure, there appear more hydrophilic centers, and the solvation (and activation) energy decreases. However, with the second water molecule, some of these hydrophilic centers disappear, and the solvation (and activation) energy increases slightly. Furthermore, our MD/ESIE produces a decrease of 3.50 kcal/mol in the activation barrier which is coherent with the work of Almatarneh et al. [16] who found a decrease of 4.83 kcal/mol with G3 level theory when passing from TS1 to TS2, there is no information available for the MP2/6-31G (d) calculation.

The clear conclusion of this work is that the free energy curves of the species involved in the reaction provide a good description of the thermodynamics of formamidine decomposition in an aqueous medium. These curves, which are constructed based on the solute–solvent interaction energies with the solvent fluctuation being chosen as reaction coordinate, respond acceptably to the activation barrier of the process. Also, to obtain reasonable results for this reaction using the geometries in solution, one must take into account a mechanism assisted with water molecules, since one observes that the activation barrier for the process decreases appreciably when water molecules are involved in the reaction. Thus, the MD/ESIE discrete solvent model predicts a significant lowering of the activation free energy by 17.36 (reaction FM + H_2O) and 20.86 (reaction FM + $2H_2O$) kcal/mol relative to the unimolecular decomposition without water. The activation barriers show that the decomposition assisted with one or two water molecules in aqueous solution is preferred over the non-assisted mechanism, achieving values in agreement with the experimental data and with other similar studies when the MD method free energy curves are used.

Acknowledgments This research was sponsored by the Consejería de Infraestructuras y Desarrollo Tecnológico de la Junta de Extremadura (Project GRU09005).

References

1. Grount RJ (1975) In: Gautier JA, Miocque M, Farnoux CC, Patai S (ed) The chemistry of amidines and imidates. Wiley, New York

2. Schaefer PC (1977) In: Rappoport Z (ed) The chemistry of the cyano group. Wiley, London
3. Hollingworth RM (1976) Environ Health Perspect 14:57–69
4. Peeters D, Leroy G, Wilante C (1997) J Mol Struct 416:21
5. Zhang Q, Bell R, Truong TNJ (1995) Phys Chem 99:592
6. Nguyen KA, Gordon MS, Truhlar DG (1991) J Am Che Soc 113:1596
7. Lim JH, Lee EK, Kim Y (1997) J Phys Chem 101:2233
8. Yamabe T, Yamashita K, Kaminoyama M, Koizumi M, Tachibana A (1984) J Phys Chem 88:1459
9. Poirier RA, Majlessi D, Zielnski TJ (1986) J Comput Chem 7:464
10. Flinn C, Poirier RA, Sokalski WA (2003) J Phs Chem A 107:11171
11. Vincent S, Mioskowski C, Lebeau L (1999) J Org Chem 64:991
12. Barker J, Jones M, Kilner M (1985) Org Mass Spectrom 20:619
13. Andres J, Krechl J, Carda M, Silla E (1991) Int J Quantum Chem 50:127
14. Andres J, Bertran J, Carda M, Krechl J, Monterde J, Silla E (1992) J Mol Struct THEOCHEM 254:465
15. Kaushik R, Rastogi RC, Ray NK (1996) Indian J Chem 35A:629
16. Almatarneh MA, Flinn CG, Poirier RA (2005) Can J Chem 83:2082
17. Nagaoka M, Okuno Y, Yamabe T (1991) J Am Chem Soc 113:769
18. Miertus S, Srcocco E, Tomasi J (1981) J Chem Phys 55:117
19. Curtiss LA, Raghavachari K (1998) Computational thermochemistry. ACS Symp Ser, Irikura K, Frurip DF (eds)
20. Tolosa S, Sansón JA, Hidalgo AJ (2007) Phys Chem A 111:339
21. Tolosa S, Corchado Martín-Romo JC, Hidalgo A, Sansón JAJ (2007) Phys Chem A 111:13515
22. Tolosa S, Sansón JA, Hidalgo AJ (2009) Phys Chem 113:1858
23. Ando K, Hynes JTJ (1997) Phys Chem B 101:10464
24. Ditchfield R, Hehre WJ, Pople JAJ (1971) Chem Phys 54:724
25. Hehre WJ, Ditchfield R, Pople JAJ (1972) Chem Phys 56:2257
26. Boys SF, Bernardi F (1970) Mol Phys 19:553
27. Tolosa S, Sansón JA, Hidalgo A (2008) Chem Phys 353:73
28. Tolosa S, Sansón JA, Hidalgo A (2002) Chem Phys Lett 357:279
29. Kitaura K, Morokuma K (1976) Int J Quantum Chem 10:325
30. Umeyama H, Morokuma K (1977) J Am Chem Soc 99:1316
31. Jorgensen WL, Tirado-Rives J (1988) J Am Chem Soc 110:1657
32. Carter EA, Hynes JTJ (1989) Phys Chem 93:2184
33. Ando K, Hynes JTJ (1995) Mol Liquids 64:25
34. Yoshirnori A, Kakitani T, Enomoto Y, Mataga N (1989) J Phys Chem 93:8316
35. Hayashi S, Ando K, Kato S (1995) J Phys Chem 99:955
36. King G, Warshel AJ (1990) Chem Phys 93:8682
37. Kuharski RA, Bader JS, Chandler D, Sprik M, Klein ML, Impey RWJ (1988) Chem Phys 89:3248
38. Tachiya M (1989) J Phys Chem 93:7050
39. Case DA, Darden TA, Cheatham ITE, Simmerling CL, Wang J, Duke RE, Luo R, Mert KM, Wang B, Pearlman DA, Crowley M, Brozell S, Tsui V, Gohlke H, Mongan J, Hornak V, Cui G, Beroza P, Schafmeister C, Caldwell JW, Schevitz RW, Kollman PA (2004) AMBER 8. University of California, San Francisco
40. Ewald P (1921) Ann Phys 64:253
41. Ryckaert P, Ciccotti G, Berendsen JJCJ (1977) Comp Phys 23:237
42. Frisch MJ, Trucks GW, Schlegel HB, Scuseria GE, Robb MA, Cheeseman JR, Zakrzewski VG, Montgomery JA Jr, Stratmann RE, Burant JC, Dapprich S, Millam JM, Daniels AD, Kudin KN, Strian MC, Farkas O, Tomas J, Barone V, Cossi M, Cammi R, Mennucci B, Pomelli C, Adamo C, Clifford S, Ochterski J, Petersson GA, Ayala PY, Cui PY, Morokuma K, Malick DK, Rabuck AD, Raghavachari K, Foresman JB, Cioslowski J, Ortiz JV, Baboul AG, Stefanov BB, Liu G, Liashenko A, Piskorz P, Komaromi I, Gomperts R, Martin RL, Fox DJ, Keith T, Al-Laham MA, Peng CY, Nanayakkara A, Gonzalez C, Challacombe M, Gill PMW, Johnson B, Chen W, Wong MW, Andres JL, Gonzalez C, Head-Gordon M, Replogle ES, Pople JA (2002) Gaussian 98, revision A.11.3. Gaussian, Inc., Pittsburgh, PA
43. Dupuis M, Spangler D, Wendoloski JGAMESS (1980) Program QG01; National resource for computations in chemistry software catalog. University of California, Berkeley, CA
44. Warshel A, Levitt MJ (1976) Mol Biol 103:227–249
45. Wesolowski TA, Warshel AJ (1993) Phys Chem 97:8050–8053
46. Wesolowski TA, Warshel AJ (1994) Phys Chem 98:5183–5187
47. Wesolowski TA, Muller RP, Warshel AJ (1996) Phys Chem 100:15444–15449
48. Luzhkov V, Warshel AJ (1992) Comput Chem 13:199–213
49. Bash PA, Field MJ, Karplus MJ (1987) Am Chem Soc 109:8092
50. Field MJ, Bash PA, Karplus MJ (1990) Comput Chem 11:700–733
51. Gao JJ (1992) Phys Chem 96:537–540
52. Gao J (1996) Rev Comp Chem 7:119
53. Gao J, Xia X (1992) Science 258:631
54. Gao J, Pavelites JJJ (1992) Am Chem Soc 114:1912
55. Gao J, Truhlar DG (2002) Ann Rev Phys Chem 53:467
56. Thery V, Rinaldi D, Rivail JL, Maigret B, Ferenczy GG (1994) J Comput Chem 15:269–282
57. Wei D, Salahub DR (1994) Chem Phys Lett 224:291–296
58. Maseras F, Morokuma K (1995) J Comp Chem 16:1170
59. Fdez Galván I, Sánchez ML, Martín ME, Olivares del Valle FJ, Aguilar MA (2003) Comput Phys Commun 155:244
60. Refson K (2000) Comput Phys Commun 126:310
61. Fdez Galván I, Martín ME, Aguilar MA (2004) J Comput Chem 25:1227
62. Halliday JD, Symons EA (1978) Can J Chem 56:1463